LA-11080-MS

C.3

Lofting of Dust by Very Large Explosions

Los Alamos

Los Alamos National Laboratory
Los Alamos, New Mexico 87545

Edited by Jody H. Heiken, INC Division

Lofting of Dust by Very Large Explosions

Allen S. Mason
David L. Finnegan
Roland C. Hagan
Robert Raymond, Jr.
George G. Cocks
William H. Zoller*
Cheryl L. Peach**

*Consultant at Los Alamos. Department of Chemistry, University of Washington, Seattle, WA
98195.
**Guest Scientist at Los Alamos. Department of Chemistry, University of Washington, Seattle,
WA 98195.

Los Alamos Los Alamos National Laboratory
Los Alamos, New Mexico 87545

LOFTING OF DUST BY VERY LARGE EXPLOSIONS

by

Allen S. Mason, David L. Finnegan, Roland C. Hagan,
Robert Raymond, Jr., George G. Cocks,
William H. Zoller, and Cheryl L. Peach

ABSTRACT

One of the goals of the Minor Scale test was to determine the quantity, form, and composition of dust lofted by a large detonation of a conventional high explosive at ground level. The explosive charge was 4427 tonnes of ammonium nitrate-fuel oil (ANFO). The experimental techniques used to determine the amount of dust were (1) use of elements in soil as natural tracers, (2) inclusion of tracer elements in the ANFO charge and the immediate surroundings, (3) airborne collection of the lofted dust on filter media, and (4) analysis of the samples for both tracers and dust. The tracer content of the sample can then relate the dust collected to the total amount lofted and to the location of its origin within the experimental setup. Indium, in the oxide form, was placed within the explosive charge, and tantalum, as very fine dust, was placed near the soil surface immediately adjacent to the charge container. The amounts of the tracers and of dust collected by each filter were measured by instrumental neutron activation analysis. A research aircraft equipped with well-characterized high-volume filter samplers was flown through the dust cloud at 10 levels between the top at 4.6 km and the bottom at 1.7 km above ground level. The cloud dust density was distinctly bimodal; its maxima were at 4.1 and 2.9 km. The majority of the indium was associated with the dust in the upper part of the cloud, and the majority of the tantalum was in the lower part. The estimate of the total dust lofted by use of the naturally occurring tracers was 3.0×10^9 g. Samples are being studied by scanning electron microscopy to determine their particle size and composition distributions as functions of location within the cloud.

I. INTRODUCTION

Surface and near-surface nuclear detonations loft dust in large amounts; a common assumption is about 0.3 Tg of dust per MT nuclear yield.[1] This dust poses problems for defense planners as well as earth scientists. In response to those problems, the Defense

1

Nuclear Agency conducts research on this and other effects by studying large detonations of conventional chemical high explosives. The test reported here used 4427 tonnes of ammonium nitrate-fuel oil mixture (ANFO) and was conducted on June 27, 1985, in the northern part of the White Sands Missile Range near Socorro, New Mexico. (Figure 1 shows the locale and its isolation. As a point of interest, this spot is only a few miles from Trinity, the site of the first nuclear detonation.) The experiment we are reporting was planned to determine the amount of dust lofted by the explosion and characterize the dust particles in terms of their size and mineralogy.

II. EXPERIMENTAL TECHNIQUE

The determination of the amount and source region of dust was based on the presence of both naturally occurring and deliberately introduced trace elements in the soil of the test area and in the explosive charge. The dust cloud was sampled by an aircraft using efficient and well-characterized filter samplers; the samples were analyzed by instrumental neutron activation analysis. The size and mineralogy of the particles were studied by removing them from the filter media, embedding them in epoxy, and producing cross sections for scanning electron microscopy.

The charge was contained in a 27-m-diam fiberglass hemisphere, into which the ANFO was loaded by air lifts that extended from ground level to the apex. The ANFO was detonated by a booster charge of 141 kg of octal located at the center of the hemisphere. The tracers introduced were 1 kg of indium oxide, placed in a polyethylene bottle about 0.5 m above the booster charge, and 10 kg of fine tantalum metal powder, placed in 20 equal portions equally spaced around the dome 3 m from its outer surface and roughly 15 cm below the ground surface.

Figure 2 shows the sampling airplane, a US Air Force WB-57F stratospheric research aircraft now on loan to NASA. It requires a crew of two: the pilot and the scientific director who operates the sampling equipment. That equipment is contained in the two large pods near the wingtips and in the duct on the lower fuselage below the right wing. The pods each house a single cellulose filter 70 cm in diameter, which is exposed to the air stream when a butterfly door at the front of the pod is opened. The duct is the external portion
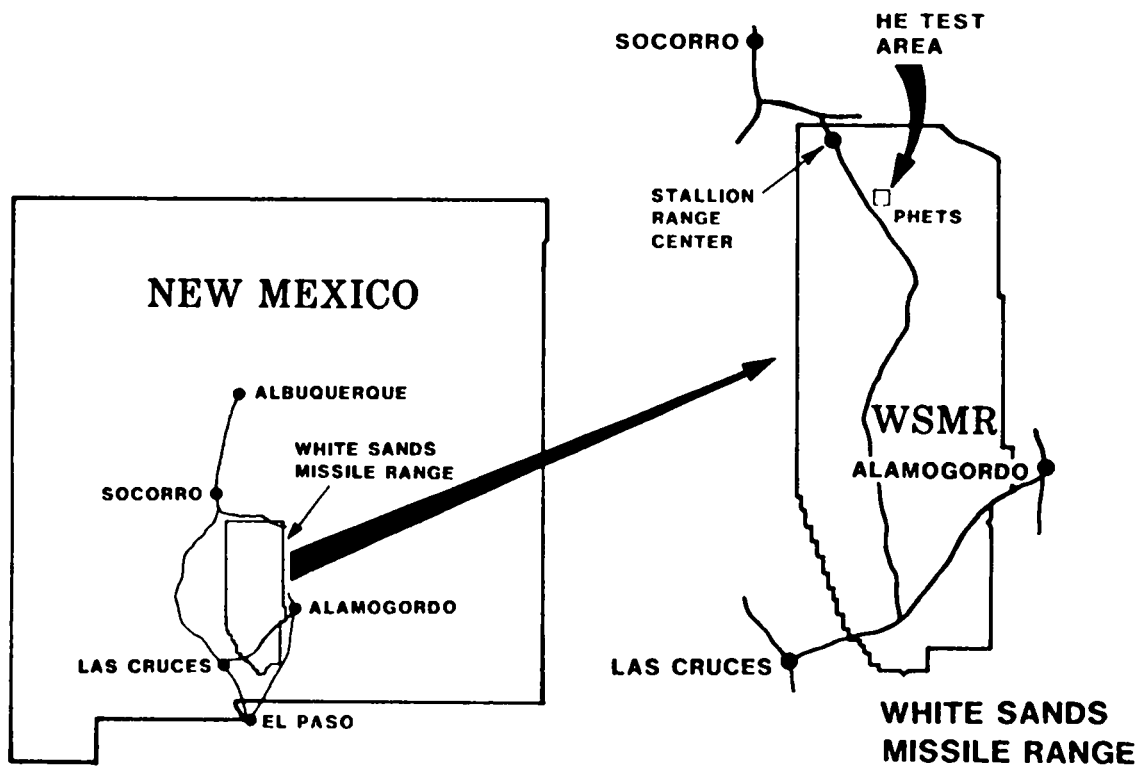
2

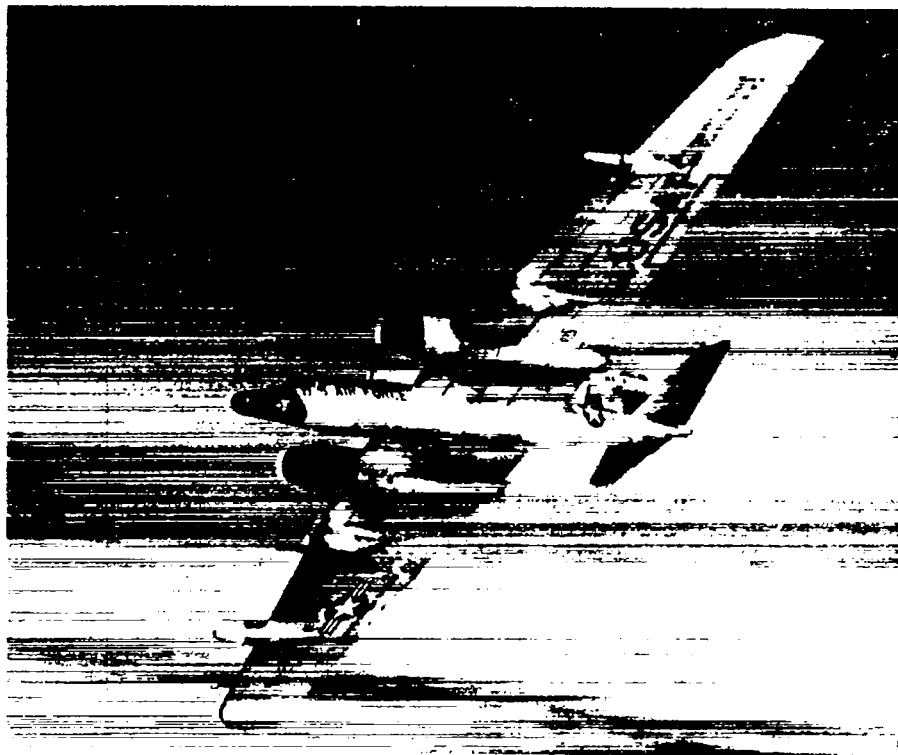Fig. 1. Location of test area.

Fig. 2. The WB-57F sampling airplane.

of a multiple sampler known as a U-1 foil. This device holds 12 filters 42 cm in diameter, which are lowered individually into the duct by remote control from the scientific director's console. The air mass flow sampled by these devices is calibrated as a function of air speed, pressure, and temperature. The air quantity sampled is then the product of the mass flow and time. In this experiment, the cloud boundaries were easily determined visually; sampling time was the elapsed time between cloud entry and exit.

Figure 3 shows the cloud as seen from the aircraft about 5 min after detonation. It has reached its maximum height of 4.6 km above the surface and is largely stable. One can see the larger particles of material falling from the bottom of the cloud. Pretest predictions indicated all debris that could seriously damage the aircraft would have fallen out after 10 min; adopting a conservative approach, we entered the cloud for the first time at 15 min. The first transit was at 150 m below the cloud top and was followed by successively lower transits at 305-m height intervals. One filter in the U-1 foil was exposed during each of 10 transits; two filters were exposed outside the cloud to serve as blanks. One pod filter was left open throughout the entire sampling period to obtain a large amount of material for analytical technique development, and the other filter was reserved against a malfunction of the U-1. No problems occurred, and the second pod was then exposed on two transits at the lowest level of the cloud. Figure 4 shows the sampling locations as vectors on a chart of the test area. We attempted to fly through the center of the visible cloud at each level, and for those levels at which the cloud was elongated, we flew along the axis.

Following the flight, the filters were cut into sixths, and opposite sixths were taken for analysis to minimize effects of airflow asymmetry within the duct. The filter segments were pressed into pellets, irradiated in the Los Alamos research reactor, and counted for activation products. The irradiation schedule was 10 s at a flux of 6×10^{12} n cm^{-2} s^{-1} followed by 5 min of decay, 300 s of counting for short-lived products, and 1200 s of counting for intermediate lifetime products. A 7.5-h irradiation with decay times of 4 and 30 days was followed by counts of 200 and 1000 min, respectively, for long-lived products. A total of 45 elements could be measured in most samples by this procedure.

Particles were separated from the filter medium by rinsing small sections (2 by 3 cm) in a mixture of 65 wt% trichlorotrifluoroethane and 35 wt% ethanol. The rinsing was followed by repeated washing and ultrasonic agitation in the same mixture and sieving to remove cotton fibers. In the last step, the particles were washed with benzene to remove the organic ester with which the cellulose filter medium was coated to improve its collection efficiency. The particles were prepared for optical and scanning electron microscopy
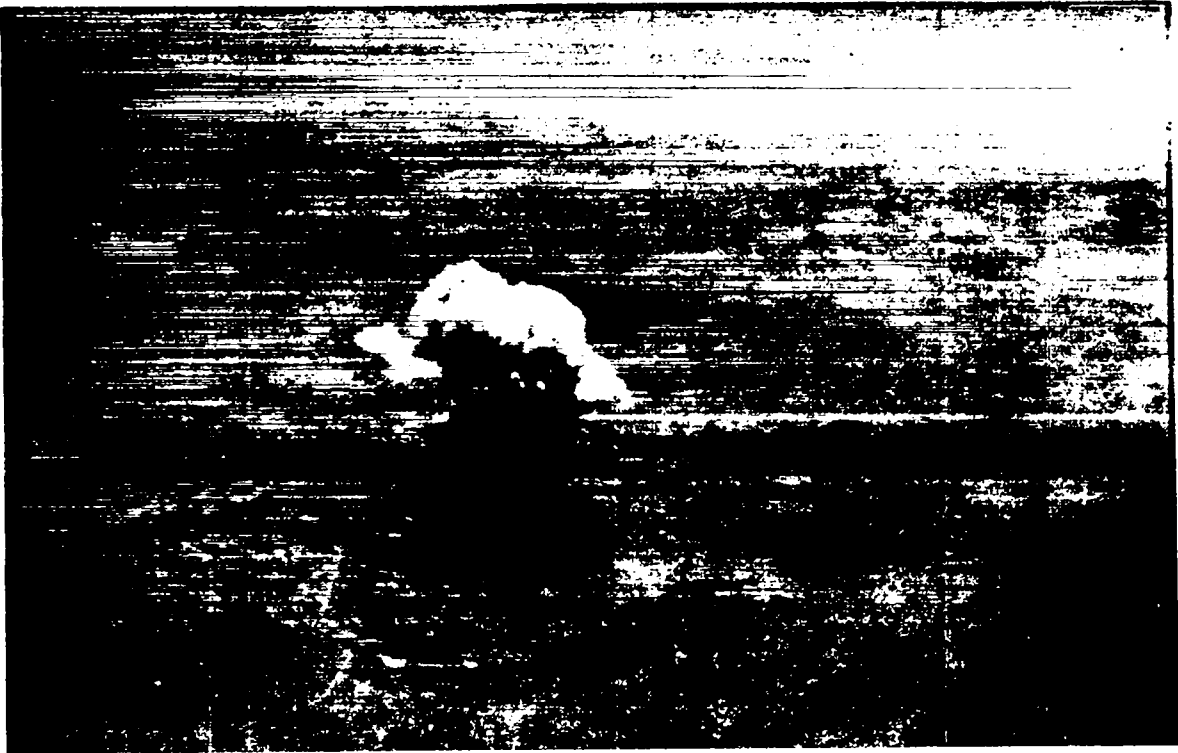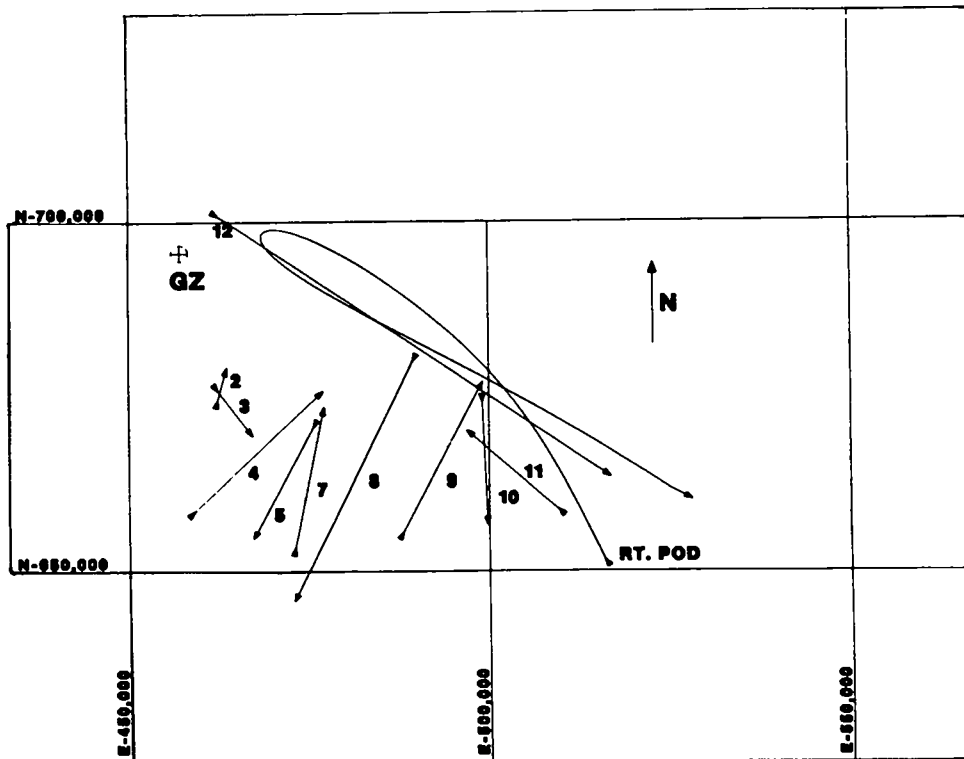
4

Fig. 3. Dust cloud at 5 min.

Fig. 4. Sampling tracks *vs* filter numbers.

by being embedded in an epoxy plastic matrix, which was then cut and polished into thin sections. Figure 5 shows sections of unused filter, heavily loaded filter, and washed filter. The efficiency of the separation technique was determined by measuring the amount of scandium and iron on segments of each of the filters, washing the segments by the above procedure, and then repeating the measurements on the washed segments. The table shows the results, which indicate that the technique is more than 90% effective.

EFFICIENCY OF THE PARTICLE-REMOVAL PROCEDURE

Filter Number	^{46}Sc Removal (%)	^{59}Fe Removal (%)
2	93.0	100.[a]
3	95.6	95.6
4	96.7	96.4
5	86.9	100.[a]
7	95.9	94.0
8	99.3	98.4
9	96.2	98.1
10	97.7	100.[a]
11	96.8	97.3
12	96.6	96.2

[a]100. indicates residual activity not detectable.

III. RESULTS

The dust mixing ratios for the ten U-1 sampler filters are shown in Fig. 6 as a function of height above ground level. Note that the maximum mixing ratio at 2.9-km height is nearly 70 ppm dust. (Dust at this mixing ratio restricts visibility to a few meters. The aircraft engines sustained no damage during this flight, probably because there was little glassy material in the dust.) These mixing ratios were obtained from the quantities of naturally occurring trace elements, typically scandium, found in the filter, the ratio of scandium to total dust found in the pretest soil samples, and the calculated air mass sampled by the filter. The bimodal distribution seen in the previous photograph is clear. A qualitative mechanism for this distribution can be inferred. The initial detonation disrupts soil in the vicinity of the charge, and the resulting dust is mixed with the very hot gaseous detonation products. The hot gases rise, carrying the dust with them. As the hot gases rise, additional dust is generated further from the charge by the radial ejection of soil
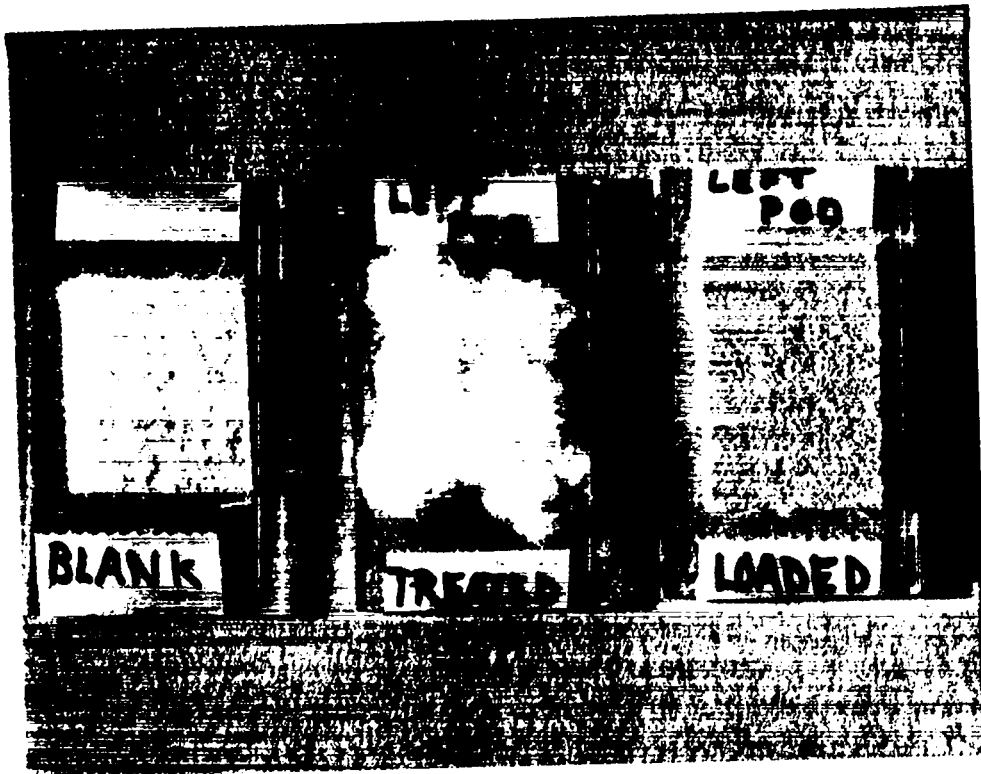
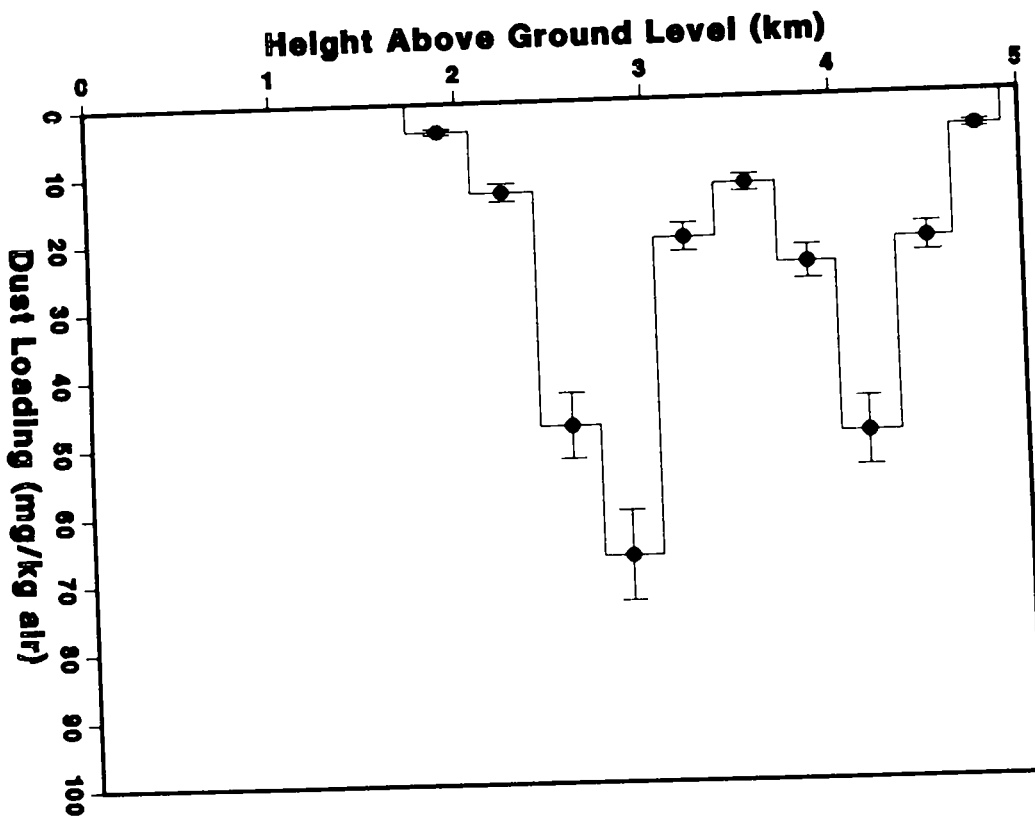Fig. 5. Blank, post-, and pre-extracted filter samples.

Fig. 6. Dust mixing ratios *vs* altitude.

during crater formation, and this dust is drawn inward and upward. The separation between the two bodies of dust is not modeled by the codes in use but is being studied. An indication of the different source regions for the two bodies of dust is seen in Fig. 7, which shows the indium mixing ratios we found. The indium is more concentrated in the upper cloud. Given the volatility of indium oxide (850°C), it is reasonable to assume that it would have vaporized and mixed with the detonation products and then condensed on dust particles from the vicinity of the charge. Indium would also be preferentially condensed on small particles because those presumably make up the majority of the available surface area and are relatively unaffected by gravitational settling in the time scale of the experiment. It should be noted that the indium content in dirt samples taken before the test in the vicinity of the charge was below our detection limit. The tantalum data are somewhat more difficult to interpret. The soil of the region contains an appreciable tantalum background that had to be subtracted from the data. The remaining mixing ratios, shown in Fig. 8, indicate a distribution more like that of the dust. This may be because the tantalum was originally placed outside the charge, but it may also be because the metal dust is more dense than the soil and consequently it settled before the sampling.

The total dust content of the cloud can be estimated from the dust mixing ratios shown above and the observed cloud dimensions. Assuming radial symmetry and considering each mixing ratio to be representative of the layer as implied by Fig. 6, it is possible to calculate a mass loading for each layer, and these figures can be added to estimate the total. Figure 9 shows the results of these calculations. To calculate the volume of the sampling area as a cylinder, the horizontal extent of each layer (cylinder diameter) is calculated from the speed of the aircraft and the time in the cloud. The height of the cylinder is the spacing between the altitudes halfway to each adjacent sample. The numbers to the left of the figure's axis are the estimates of the mass of dust in each layer (in tonnes), which total 2977. This value represents 0.37 Tg dust per MT nuclear equivalent yield. It must be kept in mind that this value does not represent a final calculation because the layer-by-layer estimates have not been adjusted to a common time, but reflect observations from detonation plus 15 min at the top to 53 min at the bottom. A final estimate will be possible when the particle-size distribution has been determined and gravitational settling can be taken into account. The numbers to the right of the axis are estimates of the quantities of indium as the element in each layer. The total of 778 g is 94% of the 827 g of indium introduced as 1 kg of the oxide. This total must be subject to the same caveat as that of the dust, with the additional complication that the indium is probably not distributed uniformly with particle mass but is strongly influenced by surface area, as discussed above.
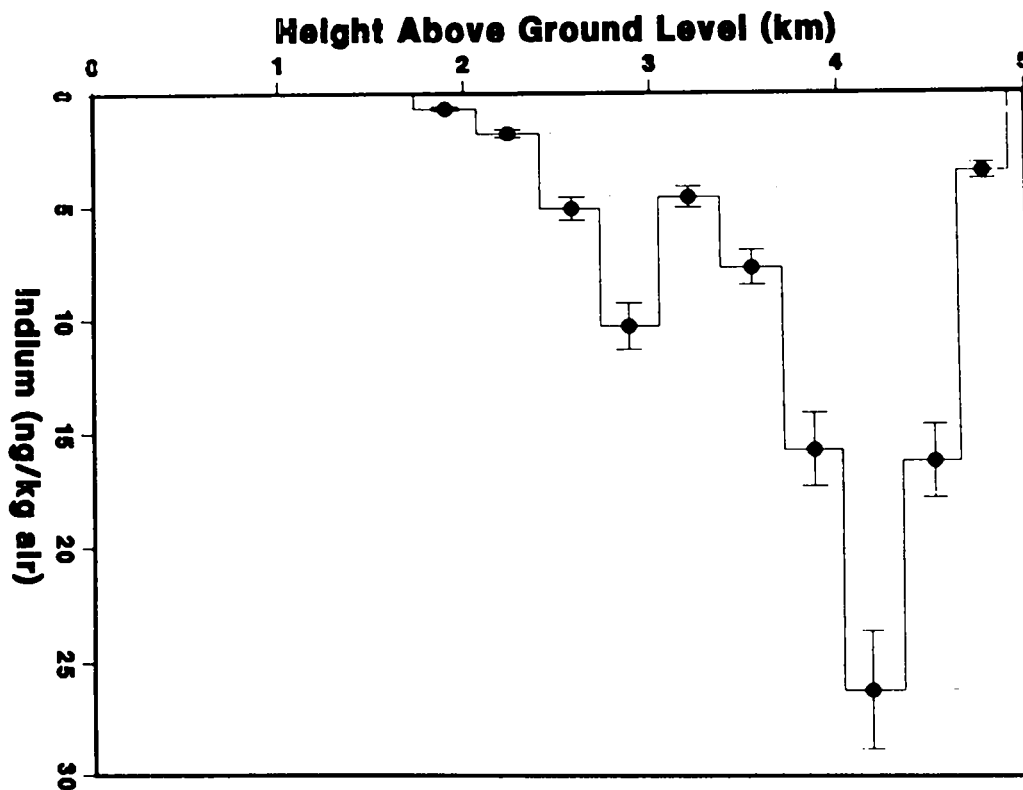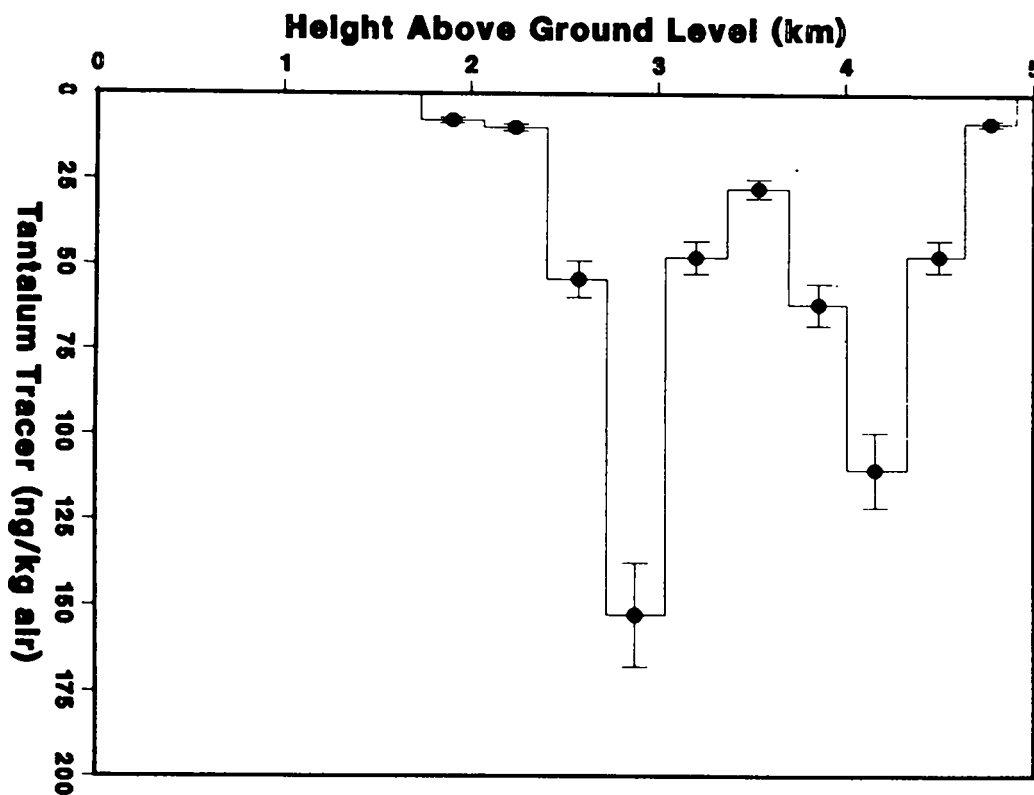
Fig. 7. Indium mixing ratios *vs* altitude

Fig. 8. Tantalum tracer (excess above background) mixing ratios *vs* altitude.

9

This apparent recovery of the original indium indicates the power of the tracer technique. This method could be employed for an experiment in which the substance of interest presented analytical difficulties, such as would be the case in measuring soot, where the introduction of a tracer would enable the calculation of mass of soot by means of the more readily determined element.

Our work on the characteristics of the individual particles is less advanced, but Fig. 10 shows an optical photomicrograph in transmitted light for a segment of the loaded cellulose filter impregnated with clear epoxy. The particles are imbedded at varying depths and are difficult to observe in the filter matrix. Optical microscopy was done on segments of this filter to characterize the particle size and distribution. Optical study appeared to indicate that the larger particles were trapped on the impact side of the filter and that smaller particles were dispersed throughout. Step scans were made across filter segments, and efforts were made to focus below the surface of the filter to count embedded particles. Optical microscopy will be developed for validating the results obtained by automated techniques discussed below, specifically to ensure that particle-size data determined by automated techniques are not biased and that particles are not altered by removal from the filter medium.

Figure 11 is a photomicrograph of a grouping of particles taken with a scanning electron microscope (SEM) in a backscattered mode. These particles were removed from the filter by the process described above, placed on a graphite mount, and coated with carbon for SEM examination. The large crystal in the upper left has an elemental composition high in potassium, aluminum, and silicon and is probably a feldspar. The aggregates of small particles show predominately calcium, aluminum, sulfur, and silicon and are probably mixtures of gypsum, calcite, and quartz. For systematic determination of particle-size distribution, it is necessary to embed the particles in epoxy in such a way as to avoid size and density segregation. The surface, on which all sizes of particles should be present, is then polished to break the particle surfaces for examination and analysis. Figure 12 is a backscatter SEM photomicrograph of the product of an experimental embedding procedure. A range of 1- to 50-μm particles is visible, as is the variation in atomic number as indicated by the apparent brightness. Three different compositions have been identified in this figure; the large, bright crystal about 50 μm in diameter (upper right) is an iron-dominant iron-titanium oxide, the weathered hexagonal crystal near the center is quartz, and the long fiber to the left of center is a shard of iron-magnesium-calcium silicate—probably a mica. All the elemental analyses are done by energy dispersive x-ray
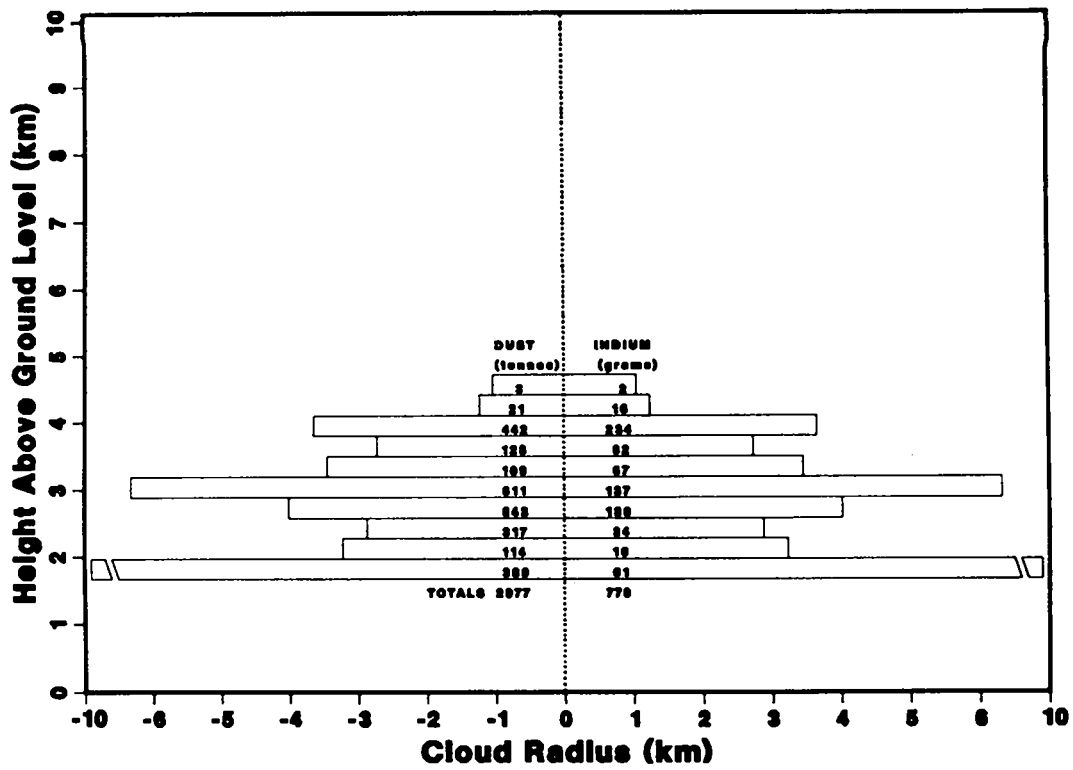
Fig. 9. Observed cloud radii *vs* altitude with estimated dust and indium inventories.
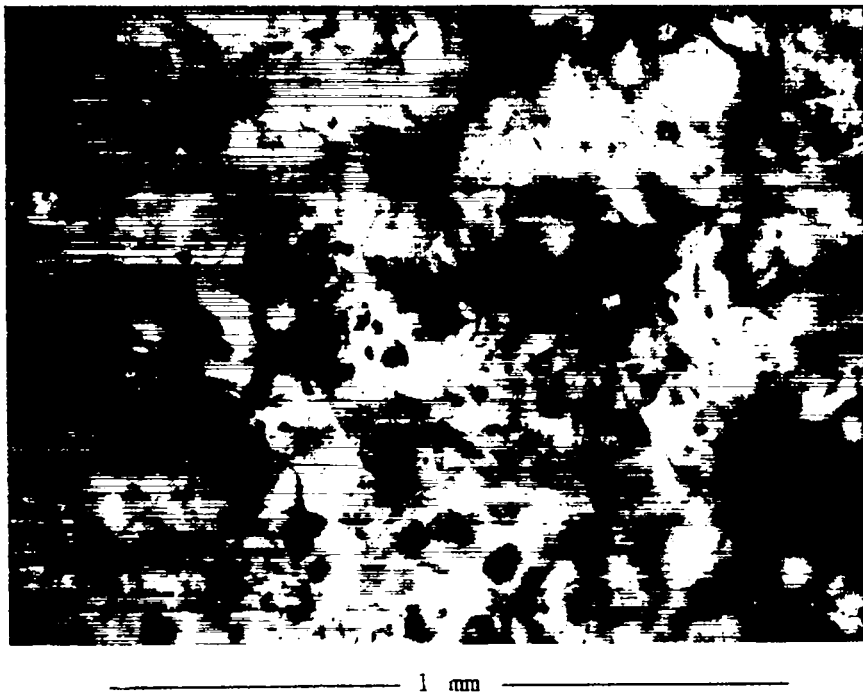

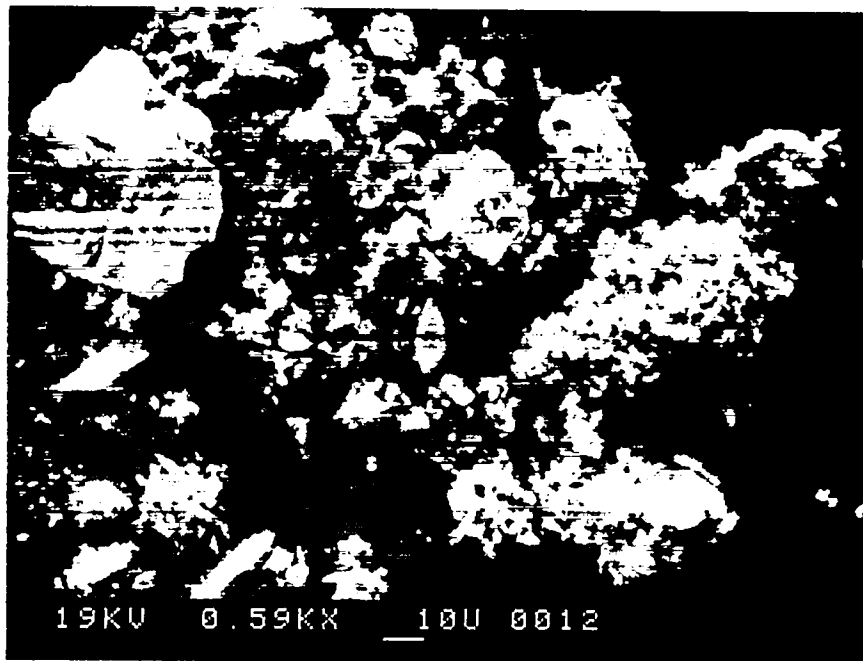Fig. 10. Optical microscopy of filter sample.
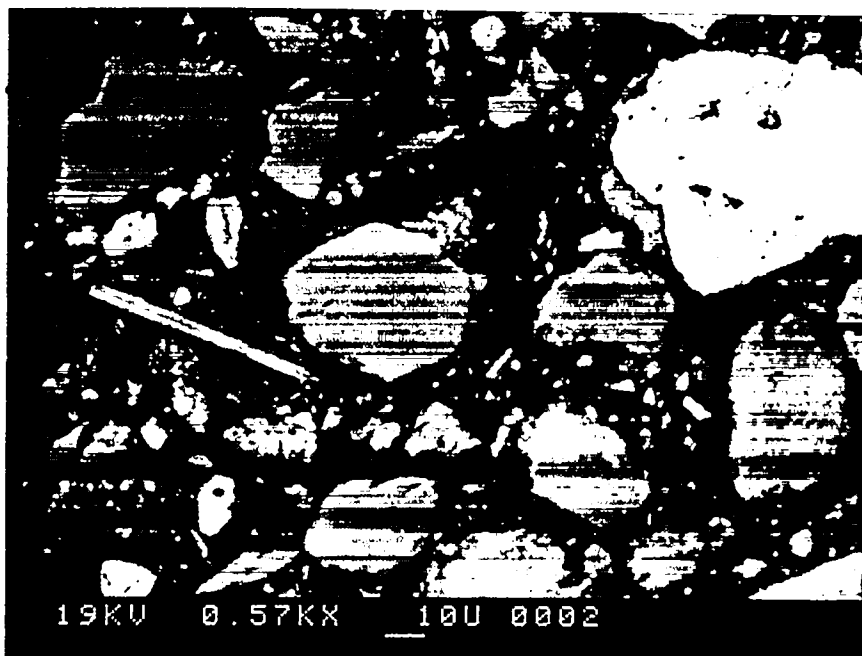
Fig. 11. The SEM photo of free particles.

Fig. 12. The photo of embedded particles.

fluorescence (EDS) with the SEM. The particle-size distribution appears at first examination to be Gaussian; there are no particles larger than 100 μm. As anticipated, there is no indication of indium, which is expected to appear as a thin coating on other particles and not in a quantity detectable by EDS. The metallic tantalum dust used as a tracer will probably be detected when the automated SEM stage is used to scan large areas of polished sections made from the various filters. This procedure will be employed to define the particle-size distribution and to determine the qualitative composition of all particles larger than 5 μm.

IV. CONCLUSIONS

The dust lofted by detonation of 4427 tonnes of chemical explosives was studied by using naturally occurring and deliberately introduced tracers. A sampling aircraft obtained filter samples at ten levels that spanned the vertical extent of the cloud. The bulk quantity of dust lofted, not corrected for gravitational settling during the time of sampling, was estimated at 0.37 Tg of dust per MT nuclear equivalent yield. The dust mixing ratios were strongly bimodal and showed substantial chemical fractionation between the upper and lower portions of the cloud.

Particles removed from the filters by ultrasonic agitation in an organic solvent mixture were studied by optical and scanning electron microscopy. Preliminary results indicate a Gaussian particle-size distribution and particle compositions representative of the terrain of the test site.

REFERENCE

1. National Research Council, *Effects on the Atmosphere of a Major Nuclear Exchange* (National Academy Press, Washington, DC, 1985).

Page Range	NTIS Price Code	Page Range	NTIS Price Code	Page Range	NTIS Price Code	Page Range	NTIS Price Code
001-025	A02	151-175	A08	301-325	A14	451-475	A20
026-050	A03	176-200	A09	326-350	A15	476-500	A21
051-075	A04	201-225	A10	351-375	A16	501-525	A22
076-100	A05	226-250	A11	376-400	A17	526-550	A23
101-125	A06	251-275	A12	401-425	A18	551-575	A24
126-150	A07	276-300	A13	426-450	A19	576-600	A25
						601-up*	A99

*Contact NTIS for a price quote.

Los Alamos